Charged particle multiplicity distributions for fixed number of jets in Z^0 hadronic decays

P. Abreu, W. Adam, F. Adami, T. Adye, G.D. Alekseev, P. Allen, S. Almehed, S.J. Alvsvaag, U. Amaldi, E. Anassontzis, et al.

EUROPEAN ORGANIZATION FOR NUCLEAR RESEARCH

CERN-PPE/92-64

15 April 1992

Charged Particle Multiplicity Distributions for Fixed Number of Jets in Z^0 Hadronic Decays

DELPHI Collaboration

Abstract

The multiplicity distributions of charged particles in full phase space and in restricted rapidity intervals for events with a fixed number of jets measured by the DELPHI detector are presented. The data are well reproduced by the Lund Parton Shower model and can also be well described by fitted negative binomial distributions. The properties of these distributions in terms of the clan model are discussed. In symmetric 3-jet events the candidate gluon jet is found not to be significantly different in average multiplicity than the mean of the other two jets, thus supporting previous results of the HRS and OPAL experiments. Similar results hold for events generated according to the LUND PS and to the HERWIG models, when the jets are defined by the JADE jet finding algorithm.The method seems to be insensitive for measuring the color charge ratio between gluons and quarks.

(Submitted to Zeits. f. Phys. C)

P.Abreu[19], W.Adam[45], F.Adami[36], T.Adye[34], G.D.Alekseev[13], P.Allen[44], S.Almehed[22], S.J.Alvsvaag[4], U.Amaldi[7], E.G.Anassontzis[3], A.Andreazza[26], P.Antilogus[23], W-D.Apel[14], R.J.Apsimon[34], B.Åsman[40], J-E.Augustin[17], A.Augustinus[28], P.Baillon[7], P.Bambade[17], F.Barao[19], R.Barate[11], G.Barbiellini[42], D.Y.Bardin[13], A.Baroncelli[37], O.Barring[22], J.A.Barrio[24], W.Bartl[45], M.J.Bates[31], M.Battaglia[26], M.Baubillier[21], K-H.Becks[47], C.J.Beeston[31], M.Begalli[33], P.Beilliere[6], Yu.Belokopytov[39], P.Beltran[9], D.Benedic[8], M.Berggren[17], D.Bertrand[2], F.Bianchi[41], M.S.Bilenky[13], P.Billoir[21], J.Bjarne[22], D.Bloch[8], S.Blyth[31], V.Bocci[35], P.N.Bogolubov[13], T.Bolognese[36], M.Bonesini[26], W.Bonivento[26], P.S.L.Booth[20], P.Borgeaud[36], G.Borisov[39], H.Borner[7], C.Bosio[37], B.Bostjancic[7], O.Botner[43], B.Bouquet[17], C.Bourdarios[17], T.J.V.Bowcock[20], M.Bozzo[10], S.Braibant[2], P.Branchini[37], K.D.Brand[32], R.A.Brenner[7], H.Briand[21], C.Bricman[2], R.C.A.Brown[7], N.Brummer[28], J-M.Brunet[6], L.Bugge[30], T.Buran[30], H.Burmeister[7], J.A.M.A.Buytaert[2], M.Caccia[7], M.Calvi[26], A.J.Camacho Rozas[38], T.Camporesi[7], V.Canale[35], F.Cao[2], F.Carena[7], L.Carroll[20], C.Caso[10], E.Castelli[42], M.V.Castillo Gimenez[44], A.Cattai[7], F.R.Cavallo[5], L.Cerrito[35], V.Chabaud[7], A.Chan[1], Ph.Charpentier[7], L.Chaussard[17], J.Chauveau[21], P.Checchia[32], G.A.Chelkov[13], L.Chevalier[36], P.Chliapnikov[39], V.Chorowicz[21], J.T.Chrin[44], R.Cirio[41], M.P.Clara[41], P.Collins[31], J.L.Contreras[24], R.Contri[10], E.Cortina[44], G.Cosme[17], F.Couchot[17], H.B.Crawley[1], D.Crennell[34], G.Crosetti[10], M.Crozon[6], J.Cuevas Maestro[38], S.Czellar[12], S.Dagoret[17], E.Dahl-Jensen[27], B.Dalmagne[17], M.Dam[30], G.Damgaard[27], G.Darbo[10], E.Daubie[2], A.Daum[14], P.D.Dauncey[31], M.Davenport[7], P.David[21], W.Da Silva[21], C.Defoix[6], D.Delikaris[7], B.A.Della Riccia[41], S.Delorme[7], P.Delpierre[6], N.Demaria[41], A.De Angelis[42], M.De Beer[36], H.De Boeck[2], W.De Boer[14], C.De Clercq[2], M.D.M.De Fez Laso[44], N.De Groot[28], C.De La Vaissiere[21], B.De Lotto[42], A.De Min[26], H.Dijkstra[7], L.Di Ciaccio[35], F.Djama[8], J.Dolbeau[6], M.Donszelmann[7], K.Doroba[46], M.Dracos[7], J.Drees[47], M.Dris[29], Y.Dufour[6], L-O.Eek[43], P.A.-M.Eerola[7], R.Ehret[14], T.Ekelof[43], G.Ekspong[40], A.Elliot Peisert[32], J-P.Engel[8], D.Fassouliotis[29], M.Feindt[7], A.Fenyuk[39], M.Fernandez Alonso[38], A.Ferrer[44], T.A.Filippas[29], A.Firestone[1], H.Foeth[7], E.Fokitis[29], F.Fontanelli[10], K.A.J.Forbes[20], B.Franek[34], P.Frenkiel[6], D.C.Fries[14], A.G.Frodesen[4], R.Fruhwirth[45], F.Fulda-Quenzer[17], K.Furnival[20], H.Furstenau[14], J.Fuster[7], G.Galeazzi[32], D.Gamba[41], C.Garcia[44], J.Garcia[38], C.Gaspar[7], U.Gasparini[32], Ph.Gavillet[7], E.N.Gazis[29], J-P.Gerber[8], P.Giacomelli[7], R.Gokieli[46], V.M.Golovatyuk[13], J.J.Gomez Y Cadenas[7], A.Goobar[40], G.Gopal[34], M.Gorski[46], V.Gracco[10], A.Grant[7], F.Grard[2], E.Graziani[37], G.Grosdidier[17], E.Gross[7], P.Grosse-Wiesmann[7], B.Grossetete[21], S.Gumenyuk[39], J.Guy[34], U.Haedinger[14], F.Hahn[7], M.Hahn[14], S.Haider[28], Z.Hajduk[15], A.Hakansson[22], A.Hallgren[43], K.Hamacher[47], G.Hamel De Monchenault[36], W.Hao[28], F.J.Harris[31], B.W.Heck[7], T.Henkes[7], J.J.Hernandez[44], P.Herquet[2], H.Herr[7], T.L.Hessing[20], I.Hietanen[12], C.O.Higgins[20], E.Higon[44], H.J.Hilke[7], S.D.Hodgson[31], T.Hofmokl[46], R.Holmes[1], S-O.Holmgren[40], D.Holthuizen[28], P.F.Honore[6], J.E.Hooper[27], M.Houlden[20], J.Hrubec[45], P.O.Hulth[40], K.Hultqvist[40], P.Ioannou[3], D.Isenhower[7], P-S.Iversen[4], J.N.Jackson[20], P.Jalocha[15], G.Jarlskog[22], P.Jarry[36], B.Jean-Marie[17], E.K.Johansson[40], D.Johnson[20], M.Jonker[7], L.Jonsson[22], P.Juillot[8], G.Kalkanis[3], G.Kalmus[34], F.Kapusta[21], M.Karlsson[7], E.Karvelas[9], S.Katsanevas[3], E.C.Katsoufis[29], R.Keranen[12], J.Kesteman[2], B.A.Khomenko[13], N.N.Khovanski[13], B.King[20], N.J.Kjaer[7], H.Klein[7], W.Klempt[7], A.Klovning[4], P.Kluit[28], J.H.Koehne[14], B.Koene[28], P.Kokkinias[9], M.Kopf[14], K.Korcyl[15], A.V.Korytov[13], V.Kostioukhine[39], C.Kourkoumelis[3], O.Kouznetsov[13], P.H.Kramer[47], J.Krolikowski[46], I.Kronkvist[22], J.Krstic[31], U.Kruener-Marquis[47], W.Krupinski[15], K.Kulka[43], K.Kurvinen[12], C.Lacasta[44], C.Lambropoulos[9], J.W.Lamsa[1], L.Lanceri[42], V.Lapin[39], J-P.Laugier[36], R.Lauhakangas[12], G.Leder[45], F.Ledroit[11], R.Leitner[7], Y.Lemoigne[36], J.Lemonne[2], G.Lensen[47], V.Lepeltier[17], A.Letessier-Selvon[21], J.M.Levy[6], E.Lieb[47], D.Liko[45], E.Lillethun[4], J.Lindgren[12], R.Lindner[47], A.Lipniacka[40], I.Lippi[32], B.Loerstad[22], M.Lokajicek[13], J.G.Loken[31], A.Lopes-Fernandes[17], M.A.Lopez Aguera[38], M.Los[28], D.Loukas[9], J.J.Lozano[44], P.Lutz[6], L.Lyons[31], G.Maehlum[7], J.Maillard[6], A.Maltezos[9], F.Mandl[45], J.Marco[38], M.Margoni[32], J-C.Marin[7], A.Markou[9], T.Maron[47], S.Marti[44], L.Mathis[1], F.Matorras[38], C.Matteuzzi[26], G.Matthiae[35], M.Mazzucato[32], M.Mc Cubbin[20], R.Mc Kay[1], R.Mc Nulty[20], G.Meola[10], C.Meroni[26], W.T.Meyer[1], M.Michelotto[32], I.Mikulec[45], W.A.Mitaroff[45], G.V.Mitselmakher[13], U.Mjoernmark[22], T.Moa[40], R.Moeller[27], K.Moenig[7], M.R.Monge[10], P.Morettini[10], H.Mueller[14], W.J.Murray[34], B.Muryn[17], G.Myatt[31], F.Naraghi[21], F.L.Navarria[5], P.Negri[26], B.S.Nielsen[27], B.Nijjhar[20], V.Nikolaenko[39], P.Niss[40], V.Obraztsov[39], A.G.Olshevski[13], R.Orava[12], A.Ostankov[39], K.Osterberg[12], A.Ouraou[36], M.Paganoni[26], R.Pain[21], H.Palka[28], Th.D.Papadopoulou[29], L.Pape[7], A.Passeri[37], M.Pegoraro[32], J.Pennanen[12], V.Perevozchikov[39], M.Pernicka[45], A.Perrotta[5], A.Petrolini[10], F.Pierre[36], M.Pimenta[19], O.Pingot[2], M.E.Pol[7], G.Polok[15], P.Poropat[42], P.Privitera[14], A.Pullia[26], D.Radojicic[31], S.Ragazzi[26], P.N.Ratoff[18], A.L.Read[30], N.G.Redaelli[26], M.Regler[45], D.Reid[20], P.B.Renton[31], L.K.Resvanis[3], F.Richard[17], M.Richardson[20], J.Ridky[13], G.Rinaudo[41], I.Roditi[16], A.Romero[41], I.Roncagliolo[10], P.Ronchese[32], C.Ronnqvist[12], E.I.Rosenberg[1], S.Rossi[7], U.Rossi[5], E.Rosso[7], P.Roudeau[17], T.Rovelli[5], W.Ruckstuhl[28], V.Ruhlmann[36], A.Ruiz[38], K.Rybicki[15], H.Saarikko[12], Y.Sacquin[36], G.Sajot[11], J.Salt[44], J.Sanchez[24], M.Sannino[10], S.Schael[14], H.Schneider[14], M.A.E.Schyns[47], G.Sciolla[41], F.Scuri[42], A.M.Segar[31], R.Sekulin[34], M.Sessa[42], G.Sette[10], R.Seufert[14], R.C.Shellard[33], P.Siegrist[36], S.Simonetti[10], F.Simonetto[32],

A.N.Sisakian[13], T.B.Skaali[30], G.Skjevling[30], G.Smadja[36,23], G.R.Smith[34], R.Sosnowski[46], T.S.Spassoff[11], E.Spiriti[37], S.Squarcia[10], H.Staeck[47], C.Stanescu[37], S.Stapnes[30], G.Stavropoulos[9], F.Stichelbaut[2], A.Stocchi[17], J.Strauss[45], J.Straver[7], R.Strub[8], M.Szczekowski[46], M.Szeptycka[46], P.Szymanski[46], T.Tabarelli[26], S.Tavernier[2], O.Tchikilev[39], G.E.Theodosiou[9], A.Tilquin[25], J.Timmermans[28], V.G.Timofeev[13], L.G.Tkatchev[13], T.Todorov[8], D.Z.Toet[28], O.Toker[12], E.Torassa[41], L.Tortora[37], M.T.Trainor[31], D.Treille[7], U.Trevisan[10], W.Trischuk[7], G.Tristram[6], C.Troncon[26], A.Tsirou[7], E.N.Tsyganov[13], M.Turala[15], M-L.Turluer[36], T.Tuuva[12], I.A.Tyapkin[13], M.Tyndel[34], S.Tzamarias[7], S.Ueberschaer[47], O.Ullaland[7], V.Uvarov[39], G.Valenti[5], E.Vallazza[41], J.A.Valls Ferrer[44], C.Vander Velde[2], G.W.Van Apeldoorn[28], P.Van Dam[28], W.K.Van Doninck[2], J.Varela[19], P.Vas[7], G.Vegni[26], L.Ventura[32], W.Venus[34], F.Verbeure[2], L.S.Vertogradov[13], D.Vilanova[36], L.Vitale[12], E.Vlasov[39], S.Vlassopoulos[29], A.S.Vodopyanov[13], M.Vollmer[47], S.Volponi[5], G.Voulgaris[3], M.Voutilainen[12], V.Vrba[37], H.Wahlen[47], C.Walck[40], F.Waldner[42], M.Wayne[1], A.Wehr[47], M.Weierstall[47], P.Weilhammer[7], J.Werner[47], A.M.Wetherell[7], J.H.Wickens[2], J.Wikne[30], G.R.Wilkinson[31], W.S.C.Williams[31], M.Winter[8], D.Wormald[30], G.Wormser[17], K.Woschnagg[43], N.Yamdagni[40], P.Yepes[7], A.Zaitsev[39], A.Zalewska[15], P.Zalewski[17], D.Zavrtanik[7], E.Zevgolatakos[9], G.Zhang[47], N.I.Zimin[13], M.Zito[36], R.Zitoun[21], R.Zukanovich Funchal[6], G.Zumerle[32], J.Zuniga[44]

[1] Ames Laboratory and Department of Physics, Iowa State University, Ames IA 50011, USA
[2] Physics Department, Univ. Instelling Antwerpen, Universiteitsplein 1, B-2610 Wilrijk, Belgium
and IIHE, ULB-VUB, Pleinlaan 2, B-1050 Brussels, Belgium
and Service de Phys. des Part. Elém., Faculté des Sciences, Université de l'Etat Mons, Av. Maistriau 19, B-7000 Mons, Belgium
[3] Physics Laboratory, University of Athens, Solonos Str. 104, GR-10680 Athens, Greece
[4] Department of Physics, University of Bergen, Allégaten 55, N-5007 Bergen, Norway
[5] Dipartimento di Fisica, Università di Bologna and INFN, Via Irnerio 46, I-40126 Bologna, Italy
[6] Collège de France, Lab. de Physique Corpusculaire, 11 pl. M. Berthelot, F-75231 Paris Cedex 05, France
[7] CERN, CH-1211 Geneva 23, Switzerland
[8] Centre de Recherche Nucléaire, IN2P3 - CNRS/ULP - BP20, F-67037 Strasbourg Cedex, France
[9] Institute of Nuclear Physics, N.C.S.R. Demokritos, P.O. Box 60228, GR-15310 Athens, Greece
[10] Dipartimento di Fisica, Università di Genova and INFN, Via Dodecaneso 33, I-16146 Genova, Italy
[11] Institut des Sciences Nucléaires, Université de Grenoble 1, F-38026 Grenoble, France
[12] Research Institute for High Energy Physics, SEFT, Siltavuorenpenger 20 C, SF-00170 Helsinki, Finland
[13] Joint Institute for Nuclear Research, Dubna, Head Post Office, P.O. Box 79, 101 000 Moscow, USSR.
[14] Institut für Experimentelle Kernphysik, Universität Karlsruhe, Postfach 6980, D-7500 Karlsruhe 1, FRG
[15] High Energy Physics Laboratory, Institute of Nuclear Physics, Ul. Kawiory 26 a, PL-30055 Krakow 30, Poland
[16] Centro Brasileiro de Pesquisas, rua Xavier Sigaud 150, RJ-22290 Rio de Janeiro, Brazil
[17] Université de Paris-Sud, Lab. de l'Accélérateur Linéaire, Bat 200, F-91405 Orsay, France
[18] School of Physics and Materials, University of Lancaster - Lancaster LA1 4YB, UK
[19] LIP, Av. E. Garcia, 14 and Inst. Sup. Te'cnico, Univ. Te'cnica de Lisboa, Av. R. Pais, P-1000 Lisbon, Portugal
[20] Department of Physics, University of Liverpool, P.O. Box 147, GB - Liverpool L69 3BX, UK
[21] LPNHE, Universités Paris VI et VII, Tour 33 (RdC), 4 place Jussieu, F-75230 Paris Cedex 05, France
[22] Department of Physics, University of Lund, Sölvegatan 14, S-22363 Lund, Sweden
[23] Université Claude Bernard de Lyon, 43 Bd du 11 Novembre 1918, F-69622 Villeurbanne Cedex, France
[24] Universidad Complutense, Avda. Complutense s/n, E-28040 Madrid, Spain
[25] Univ. d'Aix - Marseille II - Case 907 - 70, route Léon Lachamp, F-13288 Marseille Cedex 09, France
[26] Dipartimento di Fisica, Università di Milano and INFN, Via Celoria 16, I-20133 Milan, Italy
[27] Niels Bohr Institute, Blegdamsvej 17, DK-2100 Copenhagen 0, Denmark
[28] NIKHEF-H, Postbus 41882, NL-1009 DB Amsterdam, The Netherlands
[29] National Technical University, Physics Department, Zografou Campus, GR-15773 Athens, Greece
[30] Physics Department, University of Oslo, Blindern, N-1000 Oslo 3, Norway
[31] Nuclear Physics Laboratory, University of Oxford, Keble Road, GB - Oxford OX1 3RH, UK
[32] Dipartimento di Fisica, Università di Padova and INFN, Via Marzolo 8, I-35131 Padua, Italy
[33] Depto. de Fisica, Pontificia Univ. Católica, C.P. 38071 RJ-22453 Rio de Janeiro, Brazil
[34] Rutherford Appleton Laboratory, Chilton, GB - Didcot OX11 OQX, UK
[35] Dipartimento di Fisica, Università di Roma II and INFN, Tor Vergata, I-00173 Rome, Italy
[36] CEN-Saclay, DPhPE, F-91191 Gif-sur-Yvette Cedex, France
[37] Istituto Superiore di Sanità, Ist. Naz. di Fisica Nucl. (INFN), Viale Regina Elena 299, I-00161 Rome, Italy
[38] Facultad de Ciencias, Universidad de Santander, av. de los Castros, E - 39005 Santander, Spain
[39] Inst. for High Energy Physics, Serpukow P.O. Box 35, Protvino, (Moscow Region), USSR.
[40] Institute of Physics, University of Stockholm, Vanadisvägen 9, S-113 46 Stockholm, Sweden
[41] Dipartimento di Fisica Sperimentale, Università di Torino and INFN, Via P. Giuria 1, I-10125 Turin, Italy
[42] Dipartimento di Fisica, Università di Trieste and INFN, Via A. Valerio 2, I-34127 Trieste, Italy
and Istituto di Fisica, Università di Udine, I-33100 Udine, Italy
[43] Department of Radiation Sciences, University of Uppsala, P.O. Box 535, S-751 21 Uppsala, Sweden
[44] Inst. de Fisica Corpuscular IFIC, Centro Mixto Univ. de Valencia-CSIC, and Departamento de Fisica Atomica Molecular y Nuclear, Univ. de Valencia, Avda. Dr. Moliner 50, E-46100 Burjassot (Valencia), Spain
[45] Institut für Hochenergiephysik, Österr. Akad. d. Wissensch., Nikolsdorfergasse 18, A-1050 Vienna, Austria
[46] Inst. Nuclear Studies and, University of Warsaw, Ul. Hoza 69, PL-00681 Warsaw, Poland
[47] Fachbereich Physik, University of Wuppertal, Postfach 100 127, D-5600 Wuppertal 1, FRG

1 Introduction

In previous papers[1],[2] we presented an analysis of the multiplicity distributions of charged particles produced in hadronic Z^0 decays in the DELPHI detector. In particular, it was shown[2] that the multiplicity distribution reveals a shoulder structure which was shown to be well reproduced by the Lund Parton Shower (PS) model (Monte Carlo program JETSET version 6.3 and 7.2)[3],[4] and was explained by the superposition of 2-jet events with mostly low multiplicities, and 3- and 4-jet events yielding larger multiplicities.

Due to the shoulder structure the multiplicity distribution could not be described by a negative binomial distribution (NBD) which, however, has been successfully fitted in many previous experiments[5]-[14].

In this paper we extend this study and report on properties of charged particle multiplicity distributions in full phase space and in restricted intervals of rapidity for events with selected jet multiplicities. We show that the charged particle multiplicity distributions for events with a given number of jets, as well as the multiplicity distributions of individual jets for events with a given number of jets, are well described by fitted NBD's. The data are also compared with the Lund PS model and good agreement is found. An attempt is made to compare the average multiplicities for quark and gluon jets.

In Section 2 the event sample, the selection criteria and the correction procedures are described. The procedure used for the separation of multi-jet events is described in Section 3. Experimental results on charged particle multiplicity distributions for events with selected jet multiplicities and for the individual jets are presented in Sections 4 and 5. The average charged particle multiplicity of quark and gluon jets in 3-jet events is discussed in Section 5. A summary is given in Section 6.

2 Selection and Treatment of Data

This study is based on 94439 hadronic events with five or more charged particles obtained in 1989-1990 with the DELPHI detector at the LEP collider at energies near the Z^0-resonance. The DELPHI detector has been described in detail elsewhere[15]. The measurements presented here are based on charged particles detected by the Time Projection Chamber (TPC). For the event selection, we apply the same cuts as in our previous studies[1],[2]. The most important of these cuts are that a track was kept only if it extrapolated back to the nominal crossing point within 5 cm in the transverse direction and 10 cm along the beam direction, if its momentum was greater than 0.1 GeV/c, if its measured track length was greater than 50 cm and if its polar angle was between 25° and 155°. Events were kept only if the energy of charged particles (assumed to have the pion mass) in each of the two hemispheres with respect to the beam axis exceeded 3 GeV, if the total energy of charged particles exceeded 15 GeV, if there were at least 5 charged particles with momenta above 0.2 GeV/c and if the polar angle of the sphericity axis was in the range $40° < \theta < 140°$. The resulting data sample comprised 63434 events. The possible contaminations from events due to beam-gas scattering, $\gamma\gamma$ interactions and $\tau^+\tau^-$ events were reduced to a negligible level ($< 0.1\%$, $< 0.1\%$ and $< 0.15\%$, respectively) by the imposed cuts.

The corrected multiplicity distribution of the events was calculated from the observed one by means of a matrix unfolding technique described in detail in ref. [2]. The matrix was determined from a full detector simulation of 54000 events generated according to

the Lund PS model, treating the simulated tracks in the same way as the real data. This matrix can be used for correction of the observed distribution if the kinematic distributions of charged particles do not differ widely from those in the Lund PS model. We stress that the errors of the corrected multiplicity distributions are strongly correlated in nearby bins due to the method of correction. Therefore comparisons between data and models are made by transforming the predictions for the multiplicity distribution back to the level of the uncorrected data. However, in the figures we show the comparison between model predictions and corrected distributions. The correction matrix was determined for each rapidity interval under study.

3 Selection of Multi-Jet Final States

In order to study the charged particle multiplicity distributions in the different multi-jet final states we applied the jet finding algorithm originally introduced by the JADE collaboration[16]. For each event the squares of the scaled invariant masses for each pair of charged particles i and j,

$$Y_{ij} = 2E_iE_j(1-\cos\theta_{ij})/E_{vis}^2, \tag{1}$$

are evaluated. Here E_i, E_j are the energies and θ_{ij} the angle between the momentum vectors of the two particles and E_{vis} is the total energy of the charged particles in the event (pion mass assumed). The particle pair with the lowest value of Y_{ij} is selected and replaced by a pseudo-particle with four momentum $(p_i + p_j)$, thereby reducing the multiplicity by one. The procedure is repeated until the values Y_{ij} for all pairs of pseudo-particles or particles are larger than a given jet resolution Y_{min}. The remaining pseudo-particles or particles are called jets.

As is known from our previous analysis of the jet production rates at LEP energies[17], the fractions of different multi-jet configurations depend strongly on Y_{min}. For an improved understanding of jet separation, the JADE algorithm has been applied to events with initial parton $q\bar{q}$, $q\bar{q}g$, $q\bar{q}gg$ and $q\bar{q}q\bar{q}$-states generated by the JETSET 7.2 Monte Carlo program[4], with parameters optimized for the center-of-mass energy of 91 GeV[18], containing the second order QCD Matrix Elements (ME) of Ellis, Ross and Terrano[19].

The transformation of events with a certain number (m) of initial partons, as defined by the Lund ME, into events with a certain number (j) of jets, as defined by the JADE cluster algorithm applied to the generated events, can be described in terms of the transformation matrix M_{mj} (with $\sum\sum M_{mj} = 1$). The dependence of the components of M_{mj} on the jet resolution parameter Y_{min} is illustrated in Fig.1. In the Lund ME program the default value of minimum scaled invariant mass-squared of any two partons in 3- or 4-jet events, was used. Other values of the parameter were tested and they do not change the conclusions to be drawn from Fig.1. It shows that in the 2-jet events separated by the JADE algorithm, the real 2-parton states are heavily contaminated by 3- and 4-parton states even at small values of the jet resolution parameter (Fig.1a). The contamination of 3-jet events by 2- and 4-parton states is less severe at minimal values of Y_{min} up to $Y_{min} > 0.04$ (Fig.1b), while the contamination of the 4-jet sample by 2- and 3-parton states is maximal at small Y_{min} values (Fig.1c).

Next we compared the charged particle multiplicity distributions for 2-, 3- and 4-parton states generated by the Lund ME program with the ones for the same Monte Carlo events resolved into 2-, 3- and 4-jet events by the JADE algorithm. The agreement in shape of multiplicity distributions for a fixed number of initial partons and for the same number

of selected jets is reasonable at $Y_{min} = 0.005$, 0.01 and 0.02 for 2-, 3- and 4-parton(jet) states(events) respectively (as illustrated in Fig.2) but deteriorates significantly for higher values of Y_{min}.

We thus conclude that the JADE jet finding algorithm provides a reasonable separation between 2-, 3- and 4-parton events only at small values of the jet resolution parameter and the contamination of events with a given number of jets by events with different numbers of initial partons significantly affects the shape of the multiplicity distributions for $Y_{min} > 0.04$.

4 Charged Particle Multiplicity Distributions for Selected Multi-Jet States

The corrected charged particle multiplicity distributions for 2-, 3- and 4-jet events for values of the jet resolution parameter $Y_{min} = 0.01$, 0.02 and 0.04 are given in Tables 1-3 and presented in Fig.3. The errors quoted here and elsewhere are calculated from the statistical errors and from the correction procedure as described in ref. [1]. The errors are strongly correlated in nearby bins due to the method of correction.

From Fig.3 it is seen that the charged particle multiplicity distribution becomes broader and shifts to higher multiplicities as the calculated jet-multiplicity increases. This is also evident from Table 4 in which the average multiplicity $< n >$ and dispersion $D = (< n^2 > - < n >^2)^{1/2}$ for 2-, 3- and 4-jet events (together with their fractions of the total sample) are shown as a function of Y_{min}, ranging from 0.01 to 0.08. The rise of $< n >$ and D for 2- and 3-jet events with increasing Y_{min} is explained by the increasingly important contamination by events with higher parton multiplicity discussed in the preceding section (Fig.1a,b). For the 4-jet sample, the decreasing contamination by 2- and 3-jet events with increasing Y_{min} (Fig.1c) leads to a similar rise of $< n >$ with increasing Y_{min}.

The predictions of the Lund PS model are plotted together with the data in Fig.3. The model describes the data very well, apart from a slight systematic difference in the high multiplicity tail of the distributions for 2- and 3-jet events, where the Lund predictions are below the data (see also the corresponding discussion in ref. [2]). We cannot exclude the possibility that a part of this small difference is due to an imperfect treatment of the multiple photon conversion in our detector simulation program.

The charged particle multiplicity distributions for events with a fixed jet-multiplicity were fitted to the negative binomial distribution (NBD)

$$P_n(\overline{n}, k) = \frac{k(k+1)...(k+n-1)}{n!} \left(\frac{k}{k+\overline{n}}\right)^k \left(\frac{\overline{n}}{k+\overline{n}}\right)^n \qquad (2)$$

with two parameters: the average multiplicity $\overline{n}$ and the positive parameter k^{-1}, related to the dispersion D by

$$\frac{D^2}{\overline{n}^2} = \frac{1}{\overline{n}} + \frac{1}{k}. \qquad (3)$$

The fitted values of parameters are given, together with χ^2/NDF, in Table 4.

The NBD fits the multiplicity distributions for fixed numbers of jets well for values of $Y_{min} < 0.04$. The fits deteriorate for large values of Y_{min}. The deterioration of the fits for $Y_{min} \geq 0.04$ can be explained by the contamination pattern described in section 3. The

failure of the NBD to describe the overall multiplicity distribution, reported in ref. [2], seems to be related to the superposition of events with different numbers of jets. Fits of the multiplicity distributions to NBD's are shown in Fig.4 for three values of Y_{min}.

The NBD fits were also transformed to the "clan" cascading picture [20]-[22] (see also [23], [24] and refs. therein), with two parameters characterizing the clan structure: the average number of clans, $\overline{N}_c$, and the average number of charged particles per clan, $\overline{n}_c$, linked to the NBD parameters by

$$\overline{N}_c = \overline{n}/\overline{n}_c = k \cdot \ln(1 + \overline{n}/k). \tag{4}$$

The parameters $\overline{N}_c$ and $\overline{n}_c$ calculated from (4) with experimental values of $\overline{n}=< n >$ and k^{-1} are also given in Table 4. The covariance between $\overline{n}$ and k^{-1} was taken into account in calculating the errors on $\overline{N}_c$ and $\overline{n}_c$.

The mathematical property of the NBD in terms of clan parameters (Poisson distribution for the number N_c of clans and logarithmic distribution of the number of particles per clan n_c), together with the previously reported observation that the average number $\overline{N}_c$ of clans for fixed rapidity windows is approximately energy-independent both in e^+e^- annihilation and in hadronic reactions ([2] and refs. therein), is of some interest and awaits a dynamical interpretation at the parton level[23],[24]. In this respect it is also of interest that the values of $\overline{n}_c$ for events with a fixed jet multiplicity are much closer to unity (or the values of $\overline{N}_c$ are not very different from $< n >$) than for all events[2] and practically independent of the jet multiplicity.

We have also analysed the multiplicity distributions of charged particles for fixed numbers of jets and for different rapidity maxima (the rapidity y was calculated with respect to the thrust axis, assuming the pion mass for all particles). The corresponding multiplicity distributions obtained for $Y_{min} = 0.04$, together with the results of the NBD fits, are shown for illustration in Fig.5. The parameters describing the experimental distributions and the fitted NBD parameters are collected in Table 5. We find that the multiplicity distributions for 2-jet events are described by the NBD rather well in all central rapidity intervals. The fits are also good for 4-jet events, but worse for 3-jet events for $| y |< 1.0$ and $| y |< 1.5$. Fig.5b,c suggests that this can be again explained by contamination of the 3-jet sample by 2-parton events peaking at low multiplicities and, perhaps, by 4-parton events at high multiplicities. A similar behaviour is observed for other values of the jet resolution parameter Y_{min}. It is evident from Fig.5 that a shoulder structure in the multiplicity distribution, best visible in the c.m. rapidity intervals $y < 1.0$ to 2.0[2], is obviously explained by the superposition of events with different number of jets.

It is thus seen that the charged particle multiplicity distributions in restricted rapidity intervals for events with selected jet multiplicities are reasonably well described by fitted NBD's, provided that events with different jet multiplicities are well separated by the jet finding procedure. In central rapidity windows, the values of the parameter k^{-1} are significantly larger than for distributions integrated over all rapidity intervals, thus showing more important deviations of the multiplicity distributions from Poisson distributions (this is also seen in the somewhat larger values of the parameter $\overline{n}_c$). It is of interest to study the energy dependence of the NBD parameters for multiplicity distributions in the central rapidity intervals for 2-jet events. A comparison of the "clan" cascade picture parameters $\overline{N}_c$ and $\overline{n}_c$ for 2-jet events at $Y_{min} = 0.04$ with those of the HRS collaboration at $\sqrt{s} = 29$ GeV (with 2-jet events selected using sphericity and aplanarity cuts)[3] is shown in Fig.6. The average number of clans per event $\overline{N}_c$ increases almost linearly with the size of the rapidity interval in an approximately energy independent manner. The

average number of particles per clan $\overline{n}_c$ is rather constant about 1.2 at 29 GeV while at 91 GeV it increases with increasing size of the rapidity interval.

5 Average Charged Particle Multiplicity of Quark and Gluon Jets

The study of multiplicity distributions of individual jets for events with selected multi-jet configuration can provide an important insight into a possible difference between the multiplicities of quark and gluon jets.

Such a difference is predicted in the high energy limit by lowest order QCD calculations [25], [26] (see also a review [27]) which give, assuming five flavours:

$$\frac{<n>_g}{<n>_q} = \frac{9}{4}. \tag{5}$$

The value 9/4 reflects the ratio of the colour charges of the gluon and of the quark. Higher order calculations[28] modify (5) to

$$\frac{<n>_g}{<n>_q} = \frac{9}{4} \cdot (1 - 0.27\sqrt{\alpha_s} - 0.07 \cdot \alpha_s). \tag{6}$$

The expression in the brackets reduces the ratio by 10% at $\sqrt{s} = 91$ GeV. The main experimental problem is to identify the various types of jet.

In our analysis, we first defined the individual jets for a given multi-jet configuration inclusively (with 2-, 3- and 4-entries for each 2-, 3- and 4-jet event, respectively). In Table 6 we show the same parameters as in Tables 4 and 5, but evaluated for the multiplicity distributions of individual jets in events assigned to fixed multi-jet configurations. The data are shown as a function of the jet resolution parameter Y_{min}. The corresponding multiplicity distributions for several values of Y_{min} are shown for illustration in Fig.7. The distributions become narrower and shift to smaller multiplicities with increasing jet multiplicity. Fig.7 illustrates also the NBD fits to the data and the conclusions which can be drawn about these results are very similar to those made in the previous section.

Comparing the dispersions of the multiplicity distributions of the individual jets, D_i, in Table 6 with the ones for whole events, D_w, in Table 4, one notices that empirically they are approximately related by

$$D_w^2 = jD_i^2 \tag{7}$$

where j is the number of jets. This is unexpected since the full relation between the two dispersions is given by

$$D_w^2 = jD_i^2 + 2\sum\sum cov(n_k, n_l) - \sum(\overline{n}_k - \frac{\overline{n}_w}{3})^2 \tag{8}$$

where the covariance term refers to the multiplicities of pairs of jets (k, l), summed over all pairs, and where the last term is due to possible differences between the average multiplicity $(\overline{n}_k)$ of jet k from the overall average, summed over all jets. It should be noted that the dispersions appearing in these equations are invariant for changes in the labeling of the jets (such as ordering with respect to jet energy, jet multiplicity or according to the nature of the parent parton), whereas the other terms in eqn. (8) are dependent on such labeling.

If the jets are independent and with equal average multiplicities, equation (8) reduces to equation (7). If equation (7) holds, at least approximately, and since obviously the averages are related as $< n >_w = j < n >_i$, it follows that

$$\left(\frac{D_i}{< n >_i}\right) / \left(\frac{D_w}{< n >_w}\right) = \sqrt{j}. \tag{9}$$

Table 7 shows that the data in 2-, 3- and 4-jet events satisfy well this relation.[†] We conclude that there is an approximate cancellation between the term in equation (8) containing the correlations and the term measuring the lack of equality between the various average jet multiplicities, independent of the labeling of the jets. However, in the case of interest the value of each term separately is not available, since the nature of the various jets (gluon-jet or quark-jet) is unknown in the present sample.

An attempt to disentangle the quark and gluon jets in e^+e^- annihilation has previously been made by the HRS collaboration[29] by selecting symmetric 3-jet events with all jets emitted at relative angles of about 120 degrees. From their sample of 276 such events they found $< n >_g / < n >_q = 1.29^{+0.21}_{-0.41} \pm 0.20$.

A similar analysis was performed with our symmetric 3-jet event sample. Events with three jets were selected with the JADE algorithm with Y_{min}=0.01. Different choices of Y_{min} give the same result within errors. A 3-jet event is defined to be a symmetric one if the angles between every pair of jet axes, projected into the event plane, are 120 degrees with a tolerance of $\pm$20 degrees. Such events have approximately the same energy in all three jets. A reduction of the tolerance reflects in a reduction of the statistics, but does not change the conclusion. The selected sample has 451 events. For these events a fit to a NBD gives $\overline{n} = 7.54 \pm 0.15$ and k^{-1}=$(4.6 \pm 1.6) \cdot 10^{-2}$ with χ^2/NDF=8.9/18. There is no simple way to identify the gluon jet. However, it is possible to test if one of the jets has a significantly larger multiplicity than the others, thus being a candidate for a gluon jet. The jets are labeled from 1 to 3 in order of increasing multiplicity. The ratio of the average multiplicity of jet 3 to the average multiplicities of the other two, $2 \cdot < n >_3 / (< n >_1 + < n >_2)$, is found to be 1.68 ± 0.06. Because of the multiplicity ordering, this ratio is biased and must be greater than one. To quantify the expectation of the bias factor, three equal and independent jets were generated with the same NBD as found in the fit above. The bias factor is found to be 1.67. Thus the gluon candidate jet appears to have the same multiplicity as the average of the other two, in agreement with the conclusions of the HRS[29] and OPAL[31] collaborations.

This experimental finding is consistent with the expectations of the Lund PS and HERWIG[32] models where this ratio for symmetric 3-jet events selected by the JADE algorithm is predicted to be 1.64$\pm$0.06 and 1.65$\pm$0.03, respectively. If we use the completely different jet algorithm LUCLUS[4] we find the same result. The different colour charges for gluon and quarks are included in the Lund PS[33] and HERWIG[32] models, thus the method using symmetric 3-jet events as defined by the JADE algorithm seems to be insensitive to the colour charge factor at least up to about 30 GeV per jet.

Moreover, in the HERWIG model it is possible to trace each final state particle to the initial parton and thus to determine the origin of each jet. Applying this procedure to the symmetric 3-jet events, without resorting to the JADE algorithm, we find that the HERWIG gives $< n >_g / < n >_q$=1.54$\pm$0.02 and $2 < n >_3 / (< n >_1 + < n >_2)$=1.91$\pm$0.03. The value of 1.54$\pm$0.02 is substantially lower than the theoretical prediction (6), presumably because the latter is obtained by comparing the parton multiplicity produced by

[†] A similar conclusion was drawn by the OPAL collaboration[30] for events with suppressed hard gluon emission, by progressively selecting samples of events with smaller sphericity. For these clean "two-jet" events, the measured quantity (9) approaches the value of $\sqrt{2}$ as the events became more collimated.

a virtual gg system to that produced by a virtual $q\bar{q}$ one, rather than for the isolated gluon and quark jets as in our case, and also due to influence of the fragmentation and hadronization. Notice also that the value of 1.91 ± 0.03 is higher than the one obtained in the HERWIG model (as well as in the Lund PS model and in the data) for the symmetric jet events separated by the JADE algorithm. Therefore we are forced to admit that a conclusion about equal average multiplicities for gluon and quark jets in 3-jet events is not straightforward and, at least partly affected by the method of selecting jets.

6 Summary and Conclusions

The charged particle multiplicity distributions for events with selected numbers of jets have been measured in e^+e^- collisions at center-of-mass energies close to 91 GeV in the DELPHI experiment at CERN for full phase space and for central rapidity intervals. The main conclusions are:

1. The Lund Parton Shower model describes all of the studied features of the multiplicity distributions very well.

2. Negative binomial distributions can be well fitted to the multiplicity distributions for events with 2, 3 or 4 jets as well as to those of the individual jets. This result is in contrast to the very poor fit obtained to the unselected sample in ref. [2].

3. The mathematical property of the NBD in terms of clan parameters, $\overline{N}_c$ and $\overline{n}_c$, still awaits a dynamical interpretation at the parton level. For events with fixed jet multiplicity, the average number of particles per clan $\overline{n}_c$ is rather close to unity and independent of the jet multiplicity.

4. A study of symmetric 3-jet events as defined by the JADE algorithm did not reveal a different and larger average multiplicity for the gluon candidate jet as expected from the QCD at asymptotic energies. However, the method seems to be insensitive to the larger colour charge of gluons as shown by a similar treatment of events generated according to the Lund PS and the HERWIG models.

Acknowledgement. We are greatly indebted to our technical collaborators and to the funding agencies for their support in building and operating the DELPHI detector, and to the members of the CERN-SL Division for the excellent performance of the LEP collider. We thank A.Giovannini, V.Khoze and V.Petrov for stimulating discussions.

References

[1] *DELPHI Coll., P.Abreu et al.*, Z.Phys. C50(1991)185.
[2] *DELPHI Coll., P.Abreu et al.*, Z.Phys. C52(1991)271.
[3] *M.Bengtsson and T.Sjöstrand*, Phys.Lett. B185(1987)435.
[4] *T.Sjöstrand*, Comp.Phys.Comm. 27(1982)243; ibid. 28(1983)229;
T.Sjöstrand and M.Bengtsson, Comp.Phys.Comm. 43(1987)367.
[5] *UA5 Coll., G.J.Alner et al.*, Phys.Lett. B160(1985)199.
[6] *UA5 Coll., G.J.Alner et al.*, Phys.Lett. B160(1985)193.
[7] *UA5 Coll., G.J.Alner et al.*, Phys.Lett. B167(1986)476.
[8] *NA22 Coll., M.Adamus et al.*, Z.Phys. C37(1988)215; Phys.Lett. B205(1988)401.
[9] *EMC Coll., M.Arneodo et al.*, Z.Phys. C35(1987)335.
[10] *NA5 Coll., F.Dengler et al.*, Z.Phys. C33(1986)187.
[11] *NA23 Coll., J.L.Bailly et al.*, Z.Phys. C40(1988)215.
[12] *NA22 Coll., I.V.Ajinenko et al.*, Z.Phys. C46(1990)569.
[13] *HRS Coll., M.Derrick et al.*, Phys.Lett. 168B(1986)299;
Phys.Rev. D34(1986)3304.
[14] *TASSO Coll., W.Braunschweig et al.*, Z.Phys. C45(1989)193.
[15] *DELPHI Coll., P.Aarnio et al.*, NIM A303(1991)233.
[16] *JADE Coll., W.Bartel et al.*, Z.Phys. C33(1986)23; *S.Bethke et al.*, Phys.Lett. 213B(1988)235.
[17] *DELPHI Coll., P.Abreu et al.*, Phys.Lett. B247(1990)167.
[18] *W.de Boer, H.Fürstenau and J.H.Köhne*, Z.Phys. C49(1991)141.
[19] *R.K.Ellis, D.A.Ross and E.A.Terrano*, Phys.Rev.Lett. 45(1980)1226.
[20] *G.Ekspong*, Proc. XVI Intern. Symp. on Multiparticle Dynamics (Kiryat Anavim, 1985), ed. J.Grunhaus (Editions Frontieres, World Scientific, Singapore, 1985), p.309.
[21] *A.Giovannini and L.Van Hove*, Proc. XVII Intern. Symp. on Multiparticle Dynamics (Seewinkel, 1986), eds. M.Markytan et al. (World Scientific, Singapore, 1987), p.561; Z.Phys. C30(1986)391.
[22] *L.Van Hove*, Physica A147(1987)19.
[23] *A.Giovannini and L.Van Hove*, Acta Phys.Polonica B19(1988)495.
[24] *L.Van Hove and A.Giovannini*, CERN-TH.5585/90 and talk given at the 25th Int. Conf. on High Energy Physics, Singapore, 1990.
[25] *M.B.Einhorn and B.G.Weeks*, Nucl.Phys. B146(1978)445.
[26] *K.Shizuya and S.H.Tye*, Phys.Rev.Lett. 41(1978)787.
[27] *P.Mättig*, Phys.Rep. 177(1989)141.
[28] *J.B.Gaffney and A.H.Mueller*, Nucl.Phys. B250(1985)109.
[29] *HRS Coll., M.Derrick et al.*, Phys.Lett. B165(1985)449.
[30] *OPAL Coll., P.D.Acton et al.*, CERN-PPE/91-176 (1991).
[31] *OPAL Coll., G.Alexander et al.*, A direct observation of quark-gluon jet differences at LEP, CERN-PPE/91-91 (1991).
[32] *G.Marchesini et al.*, HERWIG, a Monte Carlo event generator for simulation (version 5.4), Cambridge preprint Cavendish-HEP-20/26 (DESY preprint DESY-91-048), to appear in Comp.Phys.Comm.
[33] *T.Sjöstrand*, private communication.

Table 1: Corrected charged particle multiplicity distributions $P_n \cdot 10^3$ for 2-, 3- and 4-jet events for the jet resolution parameter Y_{min}=0.01.

n	2-jets	3-jets	4-jets	n	2-jets	3-jets	4-jets
4	0.7±0.2			30	7.1±0.7	36±2	95±5
6	3.8±0.5	0.6±0.1		32	4.3±0.5	21±1	76±4
8	16±1	3.7±0.4	0.9±0.3	34	1.3±0.3	11.1±0.7	50±3
10	49±3	14.4±0.9	3.0±0.5	36	1.2±0.3	6.1±0.5	33±2
12	93±4	39±2	7.4±0.8	38	0.10±0.07	2.8±0.3	22±2
14	143±6	74±3	19±1	40	0.07±0.06	1.1±0.2	13±1
16	166±7	110±5	40±2	42		0.3±0.1	5.0±0.6
18	168±7	136±6	59±3	44		0.22±0.08	2.8±0.5
20	139±6	146±6	91±4	46		0.06±0.04	2.4±0.4
22	95±4	139±6	113±5	48			0.3±0.1
24	62±3	113±5	125±6	50			0.04±0.04
26	33±2	86±4	126±6	52			0.12±0.09
28	17±1	59±3	119±6				

Table 2: The same as in Table 1 but for Y_{min}=0.02.

n	2-jets	3-jets	4-jets	n	2-jets	3-jets	4-jets
4	0.29±0.09			30	12.5±0.8	58±3	113±6
6	2.7±0.3	0.23±0.09		32	7.4±0.6	39±2	99±6
8	11.9±0.8	2.0±0.3		34	2.8±0.3	23±1	81±5
10	38±2	8.6±0.6	2.5±0.6	36	1.2±0.2	14.3±0.9	61±4
12	80±4	23±1		38	0.6±0.1	8.0±0.6	46±3
14	126±5	49±2	8±1	40	0.07±0.05	3.9±0.4	27±2
16	154±7	82±4	14±2	42		1.5±0.2	17±2
18	163±7	109±5	25±2	44		0.8±0.2	10±1
20	146±6	129±6	52±4	46		0.4±0.1	6±1
22	110±5	136±6	83±5	48		0.13±0.06	1.7±0.5
24	75±3	124±5	102±6	50			0.8±0.4
26	43±2	106±5	119±6	52			0.9±0.4
28	26±1	82±4	131±7				

Table 3: The same as in Table 1 but for Y_{min}=0.04.

n	2-jets	3-jets	4-jets	n	2-jets	3-jets	4-jets
4	0.21±0.07			30	21±1	78±4	114±10
6	2.0±0.2			32	12.3±0.7	58±3	136±11
8	9.2±0.6	1.0±0.2		34	6.0±0.4	38±2	106±10
10	31±2	4.1±0.5		36	2.8±0.3	27±2	80±8
12	66±3	12.1±0.9		38	1.4±0.2	17±1	76±8
14	110±5	28±2	0.5±0.5	40	0.8±0.1	9.1±0.7	41±6
16	140±6	53±3	7±2	42	0.06±0.04	4.2±0.5	42±6
18	152±6	83±4	6±2	44	0.11±0.05	2.7±0.4	18±4
20	146±6	104±5	29±5	46	0.03±0.02	1.6±0.3	14±3
22	117±5	129±6	57±7	48	0.02±0.02	0.5±0.2	3±2
24	87±4	127±6	61±7	50		0.5±0.2	
26	57±3	120±5	83±8	52		0.09±0.06	3±1
28	37±2	102±5	126±11				

Table 4: Parameters characterizing the corrected multiplicity distributions for events with 2-, 3- and 4-jet configurations together with their respective fractions of the total sample, F, in dependence of the jet algorithm parameter Y_{min}, fitted values of the NBD parameters (with corresponding χ^2/NDF values) and parameters of the "clan" cascading picture.

	Y_{min}				
2-jets	0.01	0.02	0.04	0.06	0.08
$<n>$	17.6±0.7	18.4±0.7	19.3±0.8	19.8±0.8	20.2±0.8
D	4.7±0.2	5.0±0.2	5.3±0.2	5.6±0.2	5.8±0.2
F	0.282	0.463	0.659	0.767	0.834
$\overline{n}$	17.6±0.1	18.5±0.1	19.4±0.1	20.0±0.1	20.4±0.1
$k^{-1} \cdot 10^2$	1.50±0.09	1.76±0.08	2.30±0.07	2.65±0.07	2.93±0.07
χ^2/NDF	20/15	20/16	41/18	78/19	76/20
$\overline{N}_c$	15.6±0.6	15.9±0.7	15.8±0.7	15.7±0.7	15.6±0.6
$\overline{n}_c$	1.13±0.05	1.16±0.05	1.22±0.05	1.27±0.05	1.29±0.05
	Y_{min}				
3-jets	0.01	0.02	0.04	0.06	0.08
$<n>$	21.0±0.8	22.8±0.9	24.8±1.0	25.9±1.0	26.7±1.1
D	5.5±0.2	5.9±0.3	6.3±0.3	6.4±0.3	6.5±0.3
F	0.481	0.447	0.321	0.227	0.164
$\overline{n}$	21.1±0.1	22.9±0.1	24.8±0.1	26.0±0.1	26.8±0.1
$k^{-1} \cdot 10^2$	1.87±0.07	2.28±0.07	2.37±0.08	2.24±0.08	2.05±0.09
χ^2/NDF	19/18	15/18	13/20	29/20	29/20
$\overline{N}_c$	17.5±0.7	18.2±0.8	19.4±0.8	20.3±0.8	21.1±0.9
$\overline{n}_c$	1.20±0.05	1.25±0.05	1.27±0.05	1.28±0.05	1.26±0.05
	Y_{min}				
4-jets	0.01	0.02	0.04	0.06	
$<n>$	25.9±1.0	28.8±1.2	31.4±1.3	33.0±1.3	
D	6.2±0.3	6.4±0.3	6.3±0.3	5.6±0.2	
F	0.199	0.085	0.020	0.005	
$\overline{n}$	25.9±0.1	28.9±0.1	31.4±0.2	33.2±0.4	
$k^{-1} \cdot 10^2$	1.91±0.08	1.4±0.1	1.0±0.2	1.0±0.5	
χ^2/NDF	20/18	24/18	19/13	17/9	
$\overline{N}_c$	21.1±0.9	23.9±1.0	27.7±1.1	34.1±1.4	
$\overline{n}_c$	1.23±0.05	1.20±0.05	1.13±0.05	0.97±0.04	

Table 5: The same parameters as in Table 4, but for fixed value Y_{min}=0.04 of the jet resolution parameter and for different central rapidity intervals $| y | < y_{cut}$.

			y_{cut}		
2-jets	0.5	1.0	1.5	2.0	2.5
$< n >$	2.04±0.08	4.4±0.2	7.1±0.3	10.0±0.4	13.0±0.5
D	1.62±0.07	2.6±0.1	3.7±0.2	4.8±0.2	5.5±0.2
$\overline{n}$	2.03±0.02	4.36±0.02	7.10±0.03	10.1±0.03	13.1±0.04
$k^{-1} \cdot 10^2$	15.2±1.0	13.0±0.4	12.7±0.3	12.3±0.2	10.5±0.2
χ^2/NDF	9/10	31/17	48/24	70/32	28/19
$\overline{N}_c$	1.79±0.07	3.5±0.1	5.0±0.2	6.5±0.3	8.2±0.4
$\overline{n}_c$	1.14±0.05	1.26±0.05	1.40±0.06	1.55±0.06	1.59±0.07
			y_{cut}		
3-jets	0.5	1.0	1.5	2.0	2.5
$< n >$	4.9±0.2	10.0±0.4	14.6±0.6	18.3±0.7	21.3±0.9
D	2.9±0.1	4.7±0.2	6.0±0.3	6.7±0.3	6.8±0.3
$\overline{n}$	4.92±0.03	10.2±0.04	14.8±0.05	18.3±0.06	21.2±0.06
$k^{-1} \cdot 10^2$	14.6±0.5	10.3±0.2	9.2±0.2	7.7±0.1	5.7±0.1
χ^2/NDF	15/17	75/30	88/35	79/40	48/20
$\overline{N}_c$	3.7±0.2	6.6±0.3	8.9±0.4	11.3±0.5	14.0±0.6
$\overline{n}_c$	1.33±0.06	1.52±0.06	1.63±0.07	1.62±0.07	1.52±0.06
			y_{cut}		
4-jets	0.5	1.0	1.5	2.0	2.5
$< n >$	8.2±0.3	17.3±0.7	24±1	28±1	30±1
D	3.8±0.2	5.9±0.3	6.6±0.3	6.9±0.3	6.8±0.3
$\overline{n}$	8.2±0.1	17.2±0.2	24.2±0.2	28.4±0.2	30.2±0.2
$k^{-1} \cdot 10^2$	11±1	6.3±0.5	3.1±0.3	2.6±0.2	1.7±0.2
χ^2/NDF	13/16	37/24	53/27	33/28	24/15
$\overline{N}_c$	6.1±0.3	12.0±0.5	17.8±0.7	21.7±0.9	24.4±1.0
$\overline{n}_c$	1.35±0.06	1.43±0.06	1.37±0.06	1.31±0.05	1.24±0.05

Table 6: The same parameters as in Table 4, but for the multiplicity distribution of individual jets at fixed multi-jet configurations.

	Y_{min}				
2-jets	0.005	0.01	0.02	0.04	0.06
$< n >$	8.3±0.3	8.8±0.4	9.2±0.4	9.6±0.4	9.9±0.4
D	3.1±0.1	3.3±0.1	3.5±0.1	3.8±0.2	4.1±0.2
$\overline{n}$	8.29±0.04	8.78±0.03	9.21±0.03	9.70±0.03	10.0±0.03
$k^{-1} \cdot 10^2$	1.6±0.2	2.5±0.2	3.7±0.2	5.3±0.1	6.4±0.2
χ^2/NDF	13/18	24/20	27/22	59/26	86/27
$\overline{N}_c$	7.7±0.3	7.9±0.3	7.9±0.3	7.7±0.3	7.6±0.3
$\overline{n}_c$	1.07±0.04	1.11±0.05	1.17±0.05	1.25±0.05	1.31±0.05
	Y_{min}				
3-jets	0.005	0.01	0.02	0.04	
$< n >$	6.5±0.3	7.0±0.3	7.6±0.3	8.2±0.3	
D	3.0±0.1	3.2±0.1	3.4±0.1	3.7±0.2	
$\overline{n}$	6.44±0.03	7.04±0.03	7.68±0.03	8.33±0.03	
$k^{-1} \cdot 10^2$	5.7±0.3	5.8±0.2	6.5±0.2	7.3±0.2	
χ^2/NDF	18/17	32/19	44/21	49/23	
$\overline{N}_c$	5.5±0.2	5.8±0.3	6.1±0.3	6.4±0.3	
$\overline{n}_c$	1.18±0.05	1.20±0.05	1.24±0.05	1.29±0.05	
	Y_{min}				
4-jets	0.005	0.01	0.02	0.04	
$< n >$	5.8±0.2	6.5±0.3	7.2±0.3	7.8±0.3	
D	2.7±0.1	3.0±0.1	3.2±0.1	3.4±0.1	
$\overline{n}$	5.82±0.03	6.53±0.03	7.21±0.05	7.85±0.10	
$k^{-1} \cdot 10^2$	4.8±0.3	5.4±0.3	6.0±0.4	6.7±0.8	
χ^2/NDF	35/16	32/17	12/17	5/16	
$\overline{N}_c$	5.1±0.2	5.5±0.2	6.0±0.3	6.3±0.3	
$\overline{n}_c$	1.13±0.05	1.17±0.05	1.20±0.05	1.24±0.05	

Table 7:

Average multiplicity-to-dispersion ratios for the whole event, $\alpha = < n >_w / D_w$, and for individual jets, $\beta = < n >_i / D_i$, and their ratios $\gamma = \alpha/\beta$ for 2-, 3- and 4-jet events as a function of the jet resolution parameter Y_{min}.

Number of jets	Parameter	Y_{min} 0.01	0.02	0.04
2	α	3.72±0.15	3.71±0.15	3.61±0.15
	β	2.66±0.11	2.60±0.11	2.50±0.10
	γ	1.40±0.08	1.43±0.08	1.44±0.08
3	α	3.85±0.16	3.84±0.16	3.94±0.16
	β	2.21±0.09	2.23±0.09	2.24±0.09
	γ	1.74±0.10	1.72±0.10	1.76±0.10
4	α	4.17±0.17	4.48±0.18	4.95±0.21
	β	2.18±0.09	2.24±0.09	2.28±0.09
	γ	1.91±0.11	2.00±0.11	2.17±0.13

Figure Captions

Figure 1 Components of the transformation matrix M_{mj} for events with initial 2-, 3- and 4-parton states, generated by the Lund ME, into events with *a*) 2, *b*) 3 and *c*) 4 jets separated by the JADE jet finding algorithm as a function of the jet resolution parameter Y_{min} ($\sum\sum M_{mj} = 1$ for each Y_{min}). The curves are labelled with the indices (mj) of the components shown.

Figure 2 Charged particle multiplicity distribution for events with initial *a*) 2-, *b*) 3- and *c*) 4-parton states generated by the Lund ME and for the same Lund ME Monte Carlo events with *a*) 2, *b*) 3 and *c*) 4 jets separated by the JADE algorithm for the values of the jet resolution parameter $Y_{min} = 0.005$, 0.01 and 0.02, respectively.

Figure 3 Corrected charged particle multiplicity distributions for 2-, 3- and 4-jet events for several values of the jet resolution parameter *a*) $Y_{min} = 0.01$, *b*) $Y_{min} = 0.02$ and *c*) $Y_{min} = 0.04$ in comparison with the Lund PS model predictions.

Figure 4 Corrected charged particle multiplicity distributions for 2-, 3- and 4-jet events multiplied by the fraction, $F(j)$, of events assigned to the given jet configuration ($\sum P(n)F(j) = 1$) for *a*) $Y_{min} = 0.01$, *b*) $Y_{min} = 0.02$ and *c*) $Y_{min} = 0.04$. The solid curves represent fits of the data by the NBD.

Figure 5 Same as in Fig.4, but for one value of $Y_{min} = 0.04$ and for different central rapidity intervals.

Figure 6 *a*) Average number of clans, $\overline{N}_c$, *b*) Average number of charged particles per clan, $\overline{n}_c$, all obtained from the data for $Y_{min} = 0.04$, as a function of the limit of the rapidity interval.

Figure 7 Corrected charged particle multiplicity distributions of individual jets for 2-, 3- and 4-jet events multiplied by fraction, $F(j)$, of the given jet-configuration ($\sum P(n)F(j) = 1$) for *a*) $Y_{min} = 0.01$, *b*) $Y_{min} = 0.02$ and *c*) $Y_{min} = 0.04$. The solid curves represent fits of the data by the NBD.

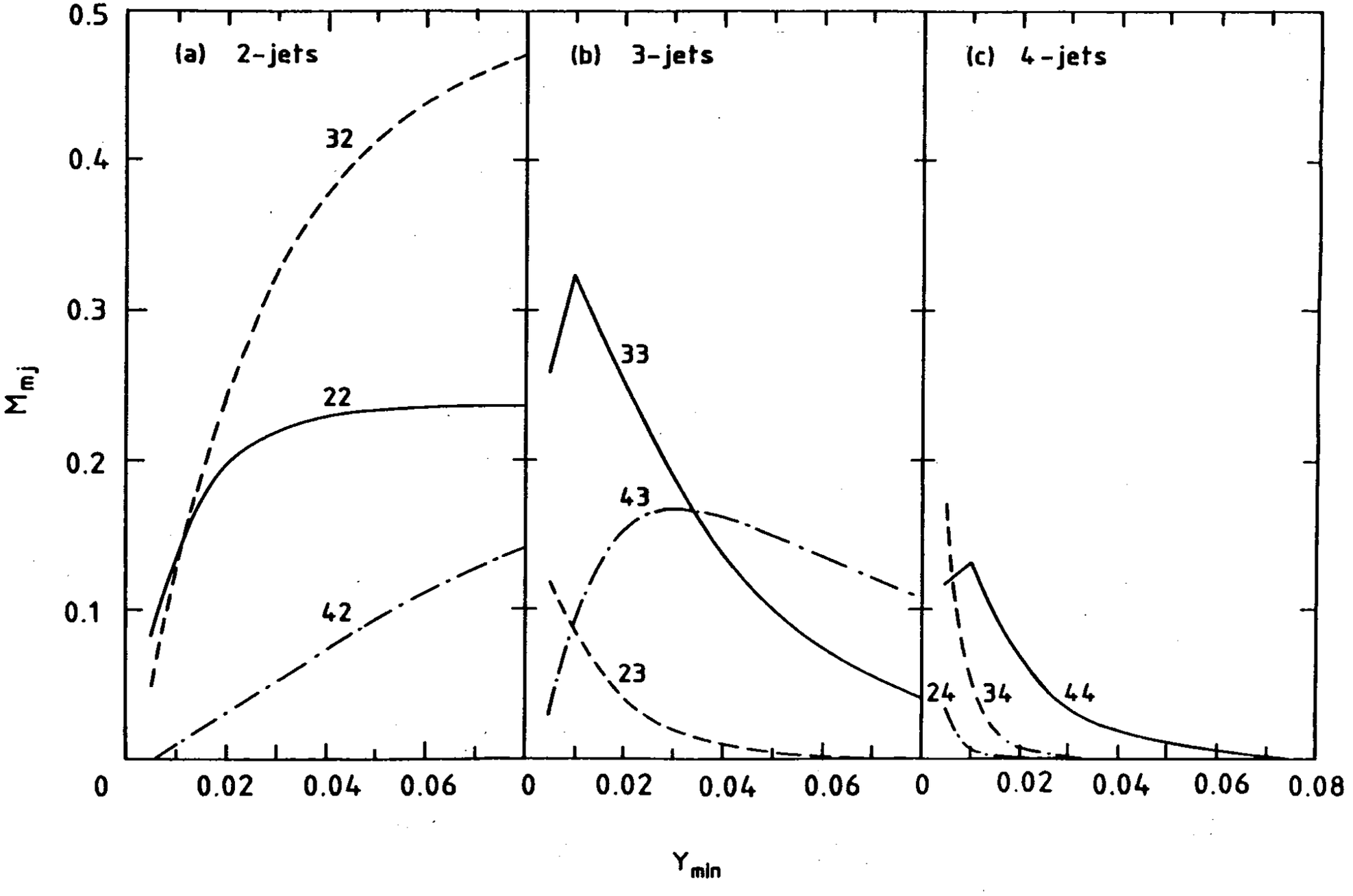
(a) 2-jets
(b) 3-jets
(c) 4-jets
32
22
42
33
43
23
24
34
44
0.5
0.4
0.3
0.2
0.1
0
0.02
0.04
0.06
0.08
Σ_{mj}
Y_{min}

Fig. 1

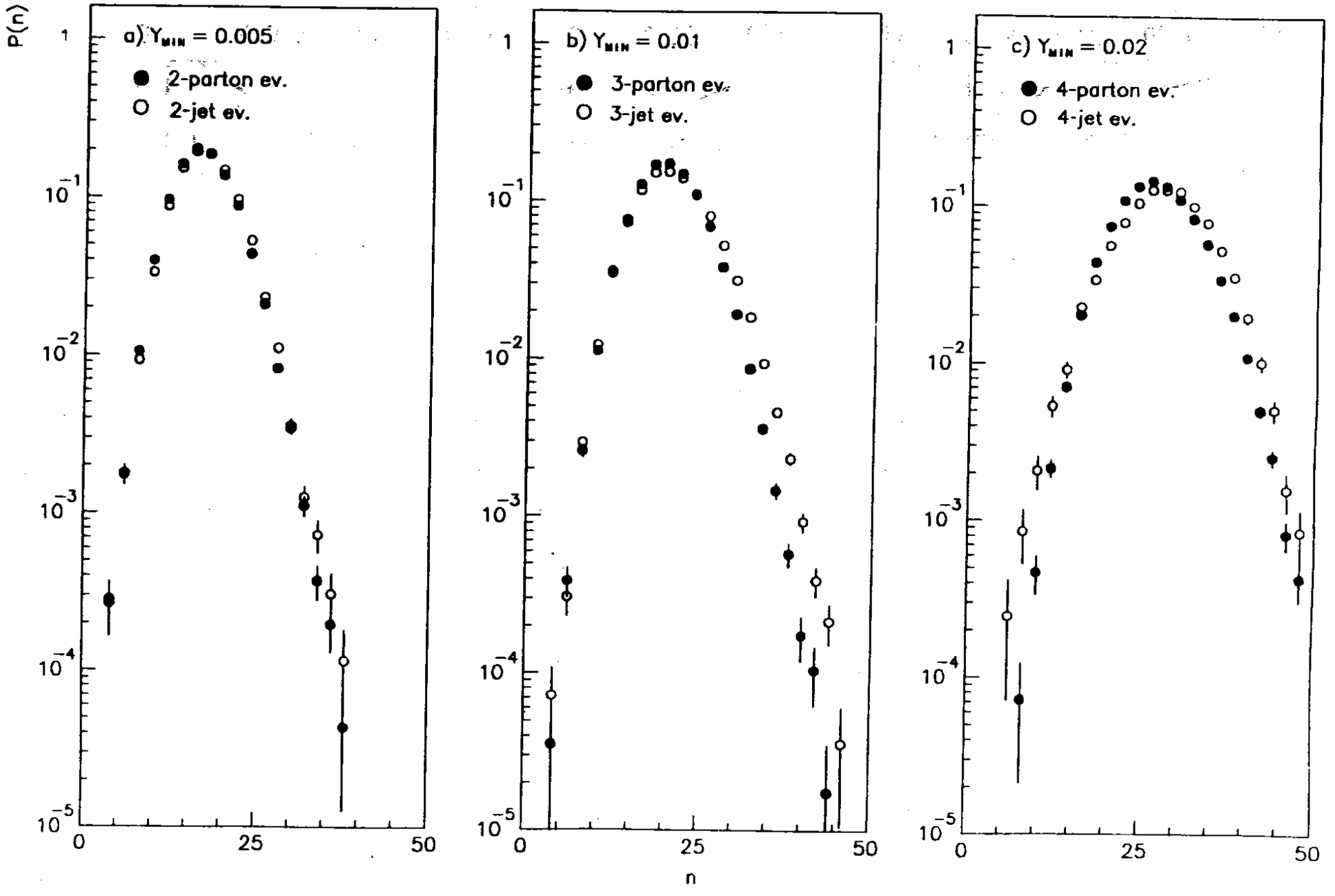
P(n)
a) Y_{MIN} = 0.005
2-parton ev.
2-jet ev.
b) Y_{MIN} = 0.01
3-parton ev.
3-jet ev.
c) Y_{MIN} = 0.02
4-parton ev.
4-jet ev.
1
10^{-1}
10^{-2}
10^{-3}
10^{-4}
10^{-5}
0
25
50
n

Fig.2

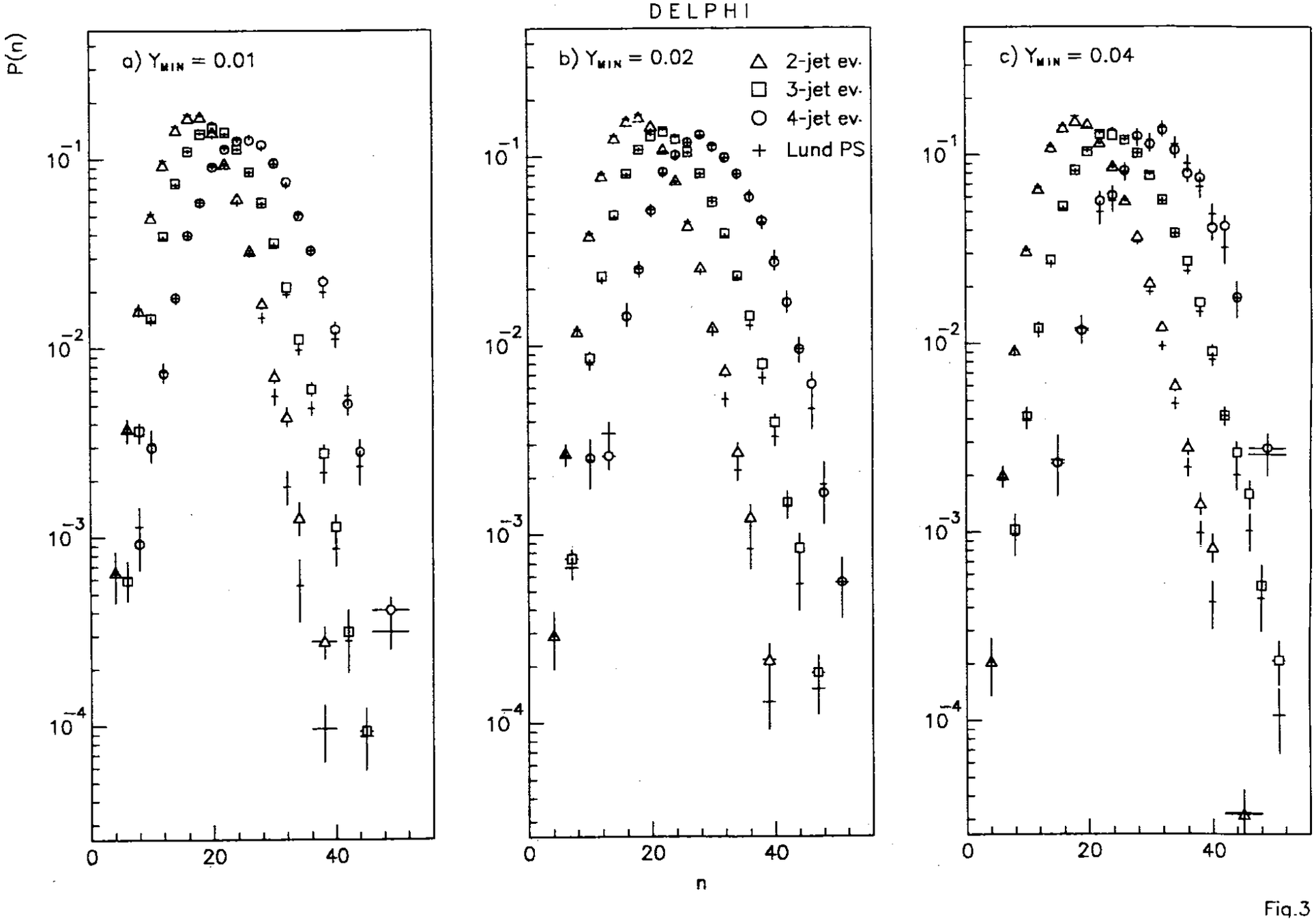
DELPHI
P(n)
a) Y_{MIN} = 0.01
b) Y_{MIN} = 0.02
c) Y_{MIN} = 0.04
2-jet ev.
3-jet ev.
4-jet ev.
Lund PS
10^{-1}
10^{-2}
10^{-3}
10^{-4}
0
20
40
n

Fig.3

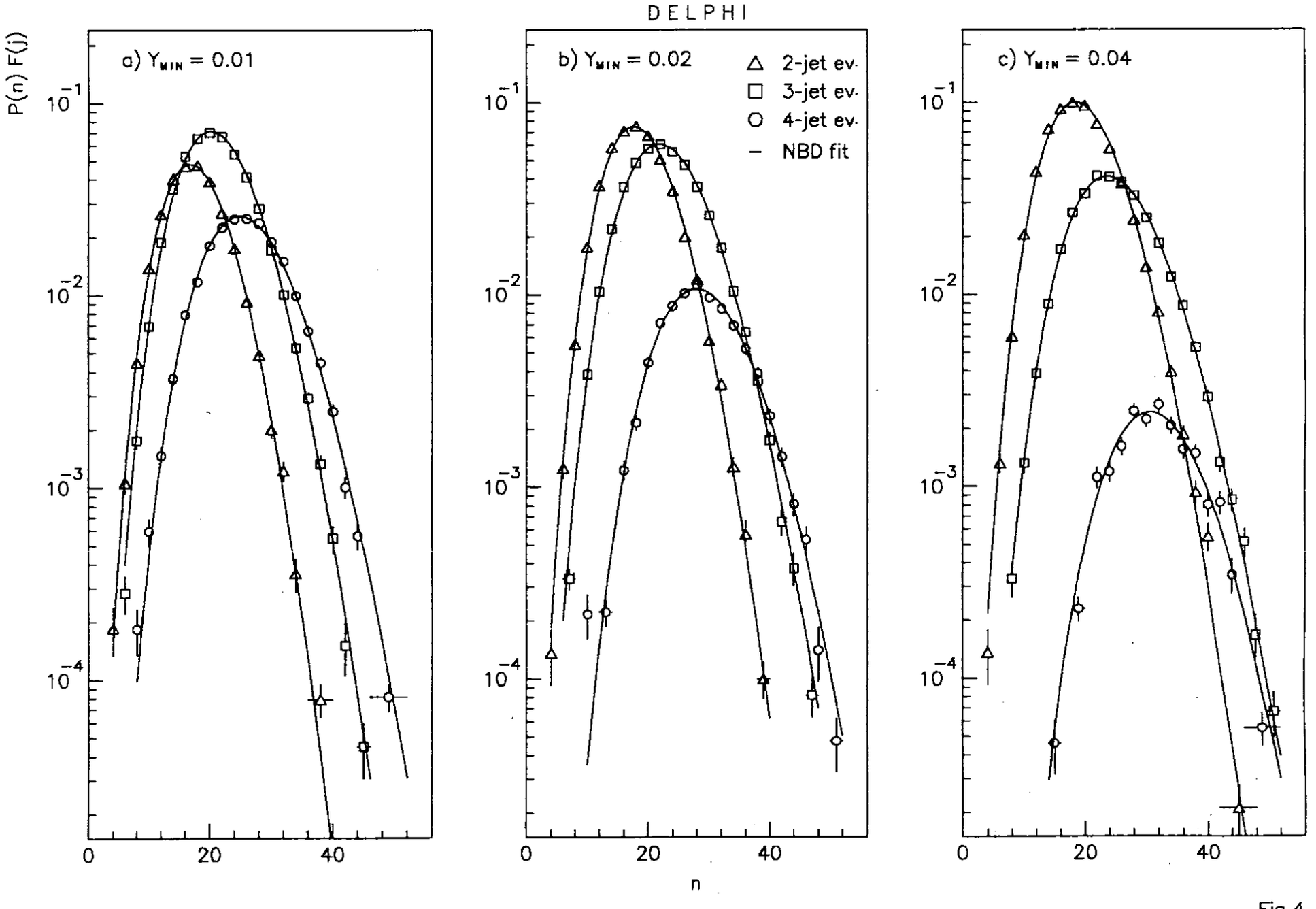
DELPHI
P(n) F(j)
a) Y_{MIN} = 0.01
b) Y_{MIN} = 0.02
c) Y_{MIN} = 0.04
2-jet ev.
3-jet ev.
4-jet ev.
NBD fit
n

Fig.4

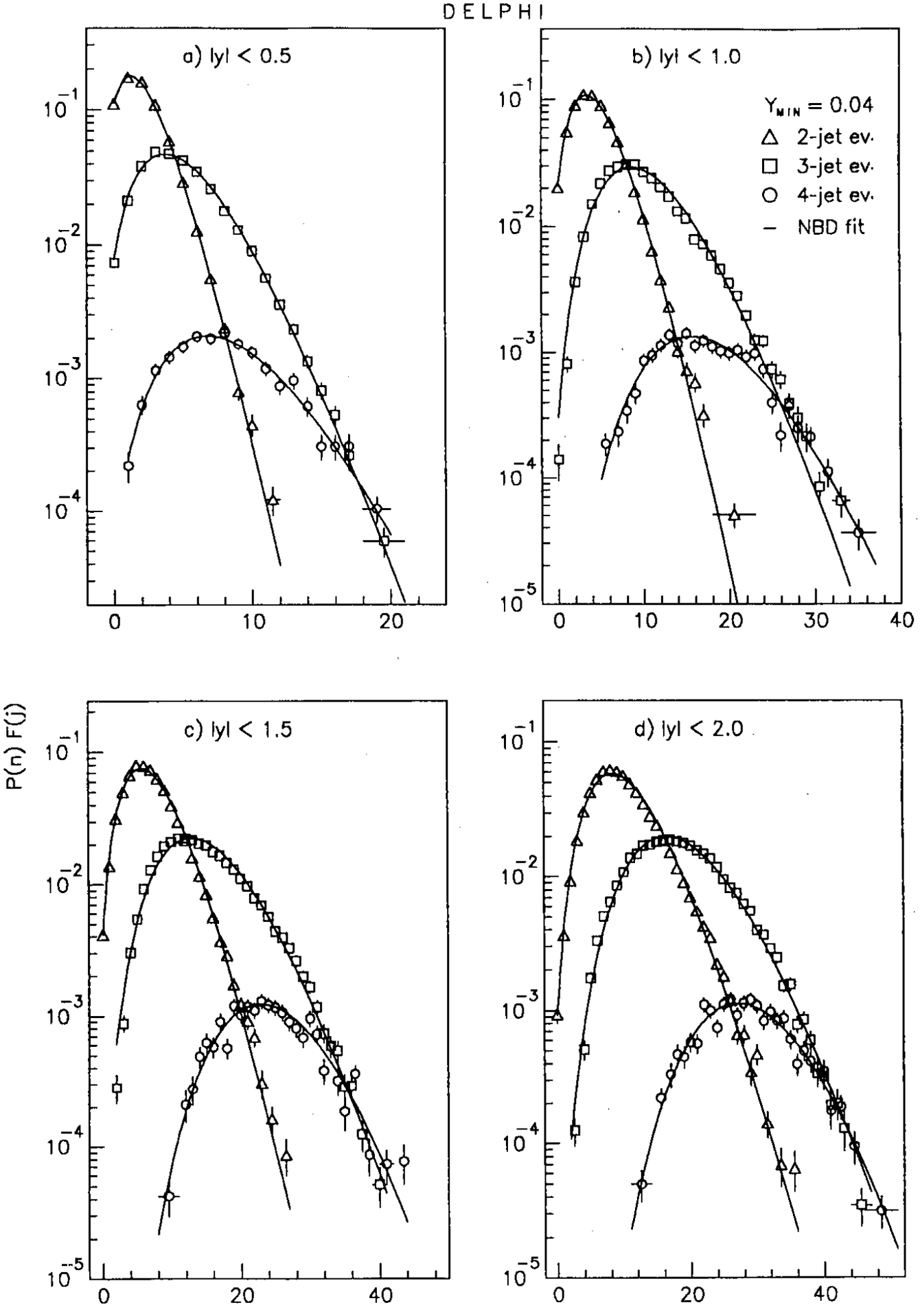
DELPHI
a) |y| < 0.5
b) |y| < 1.0
c) |y| < 1.5
d) |y| < 2.0
Y_{MIN} = 0.04
2-jet ev.
3-jet ev.
4-jet ev.
NBD fit
P(n) F(j)
n

Fig.5

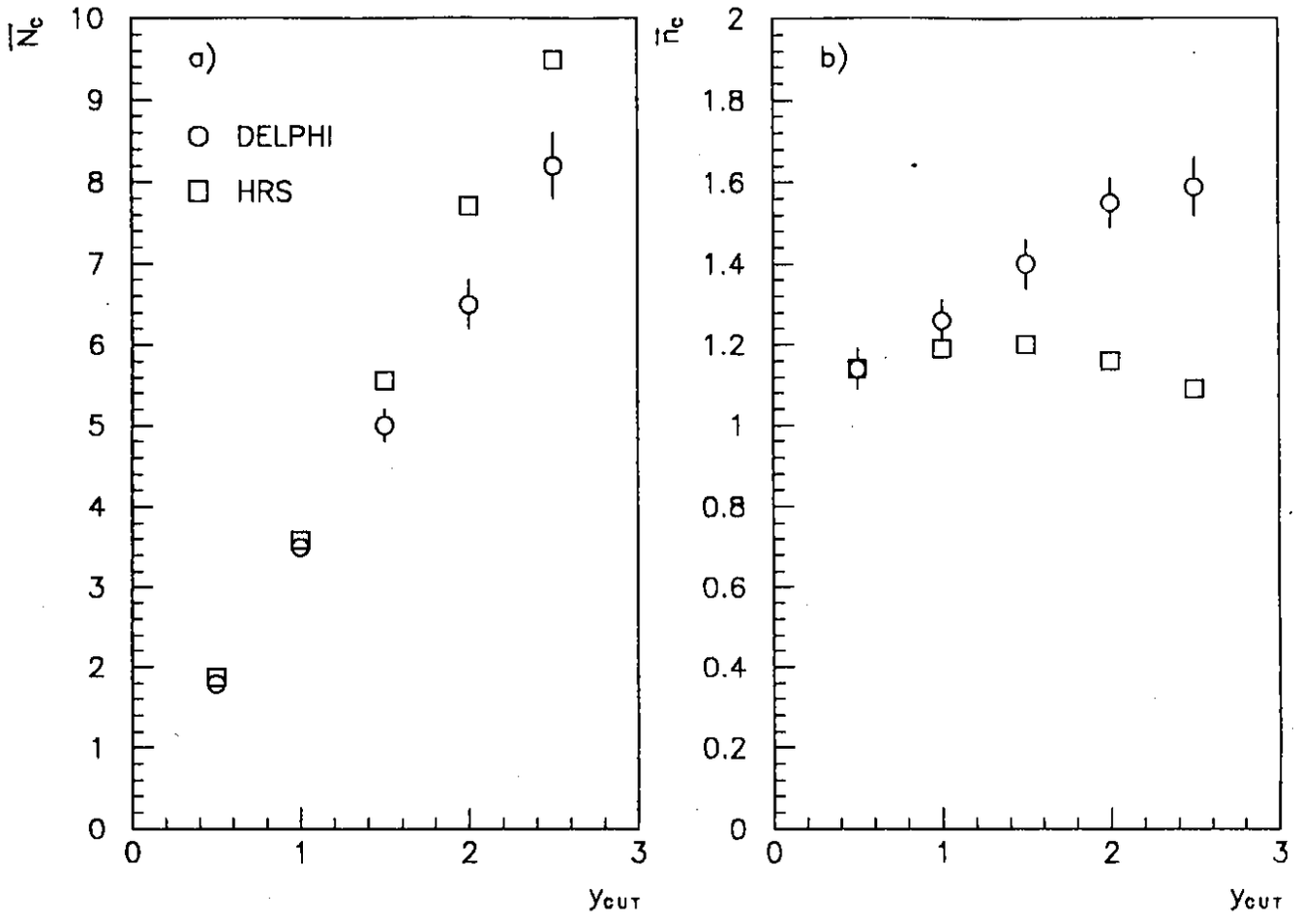

Fig.6

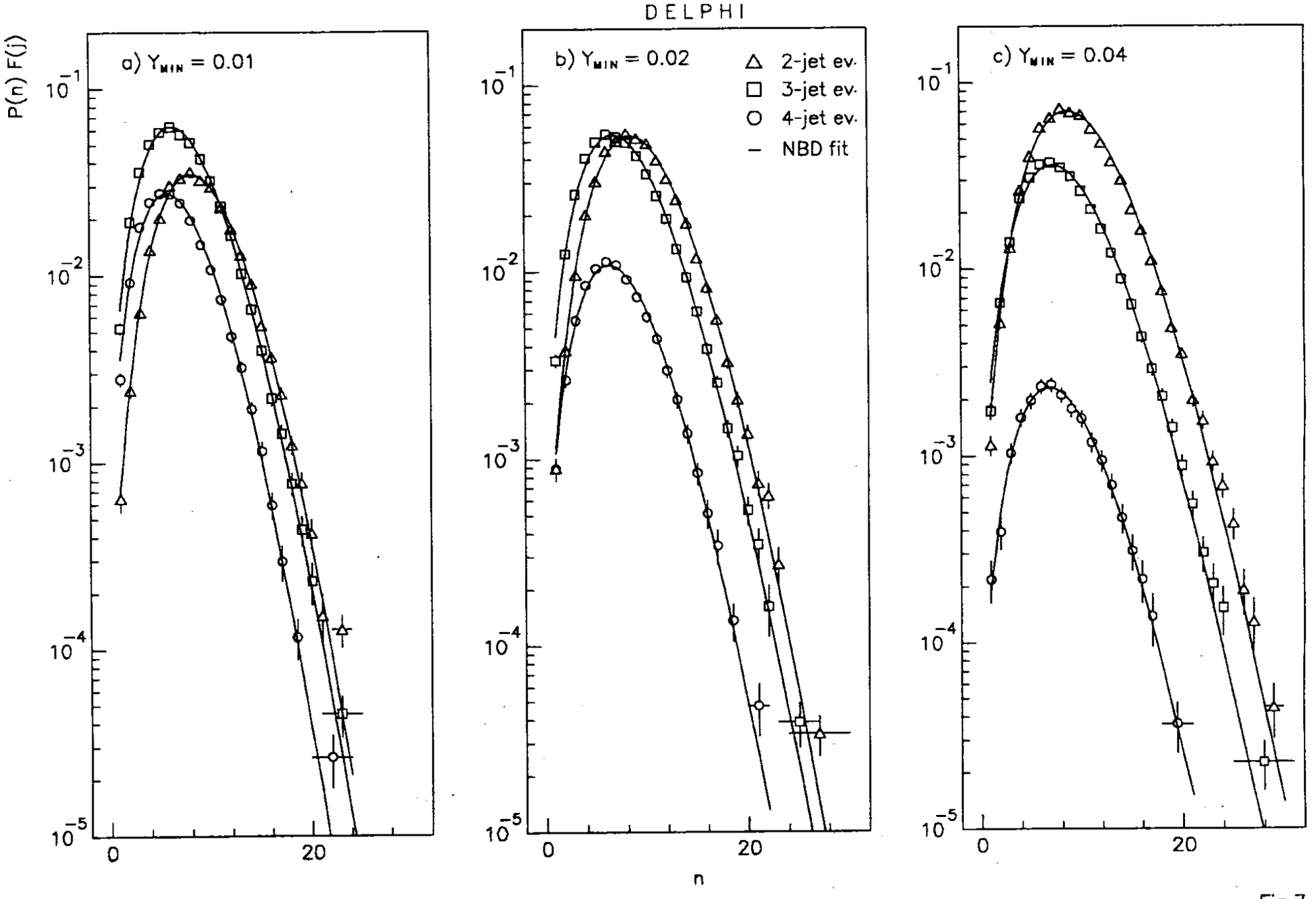
DELPHI
P(n) F(j)
a) Y_{MIN} = 0.01
b) Y_{MIN} = 0.02
c) Y_{MIN} = 0.04
2-jet ev.
3-jet ev.
4-jet ev.
NBD fit
10^{-1}
10^{-2}
10^{-3}
10^{-4}
10^{-5}
0
20
n

Fig.7